JOURNAL OF NATURAL PRODUCTS

pubs.acs.org/jnp

Article

Metabolome of the *Phyllidiella pustulosa* Species Complex (Nudibranchia, Heterobranchia, Gastropoda) Reveals Rare Dichloroimidic Sesquiterpene Derivatives from a Phylogenetically Distinct and Undescribed Clade

Alexander Bogdanov,[#] Adelfia Papu,[#] Stefan Kehraus, Max Cruesemann, Heike Wägele, and Gabriele M. König*

Cite This: https://dx.doi.org/10.1021/acs.jnatprod.0c00783

Read Online

ACCESS | Metrics & More | Article Recommendations | Supporting Information

ABSTRACT: Phyllidiid nudibranchs are brightly colored gastropod mollusks, frequently encountered in coral reefs of the tropical Indo-Pacific. The lack of a protective shell is suggested to be compensated by toxic secondary metabolites that are sequestered from specific prey sponges. Our ongoing reconstruction of phyllidiid phylogeny using molecular data of more than 700 specimens, based on published data and newly collected specimens in various seasons and localities around North Sulawesi (Indonesia), demonstrates that *Phyllidiella pustulosa* is a species complex with at least seven well-supported clades. A metabolomic analysis of 52 specimens from all seven clades of *P. pustulosa* was performed. Secondary metabolite profiles were found to correlate with the phylogenetic study and not the prevailing food sponges as expected. GNPS molecular networking revealed a unique chemotype in clade 6. Detailed chemical analysis of a specimen from this chemically and genetically distinct *P. pustulosa* clade led to the identification of seven new sesquiterpenoids with a rare dichloroimidic moiety (**1** and **4**) and derivatives thereof (**2**, **3**, **5**–**7**). Our findings suggest that *P. pustulosa* clades should be raised to the species level.

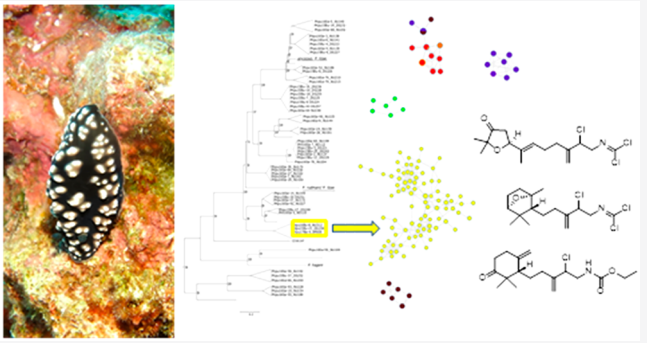

Indonesia is a famous hotspot of biodiversity and the focus of a project aiming to monitor the diversity of one group, the marine Heterobranchia (Gastropoda, Mollusca). One of the most prominent features of mollusks is their shell, which mainly serves as a protection against predators. However, reduction or complete loss of the shell is common in several molluscan groups and well known for the gastropod taxon Heterobranchia. Within this group, the marine forms, formerly known as Opisthobranchia, are well investigated with regard to alternative defense systems. These comprise a variety of strategies, including the presence of calcareous spicules, incorporation of cnidocysts from their prey, and the uptake or *de novo* biosynthesis of chemicals.[1−7] Chemical defense is considered a driving force for speciation in heterobranchs[8,9] and may explain the extraordinarily high species numbers in certain groups, such as the nudibranch family Chromodoridae (Nudibranchia, Anthobranchia) with probably more than 500 species.

Chromodorididae are sponge feeders, as are members of the anthobranch family Phyllidiidae, of which only ca. 75 species are known. Recent analyses by molecular means have shown that this latter group probably has a much higher diversity than previously assumed. Stoffels and co-workers[10] indicated that *Phyllidiella pustulosa*, one of the most common nudibranchs in tropical to temperate waters of the Indo-Pacific,[11] actually comprises several species.

Many investigations focused on secondary metabolites across the phyllidiid taxa, e.g., *Phyllidia coelestis*,[12,13] *P. ocellata*,[14,15] *P. (Fryeria) picta*,[16] *P. varicosa*,[17,18] and *Phyllidiopsis krempfi*.[19] *P. pustulosa* has been studied to the largest extent.[19−26] As a result of these studies, a large number of various sesqui- and diterpene-type secondary metabolites, mostly substituted with isocyanate and isothiocyanate functionalities, have been described. The reviews by Garson and Simpson[27] and the more recent one by Emsermann et al.[28] provide comprehensive overviews on the structural diversity of this large compound family. Chemical variability was already

Received: July 15, 2020

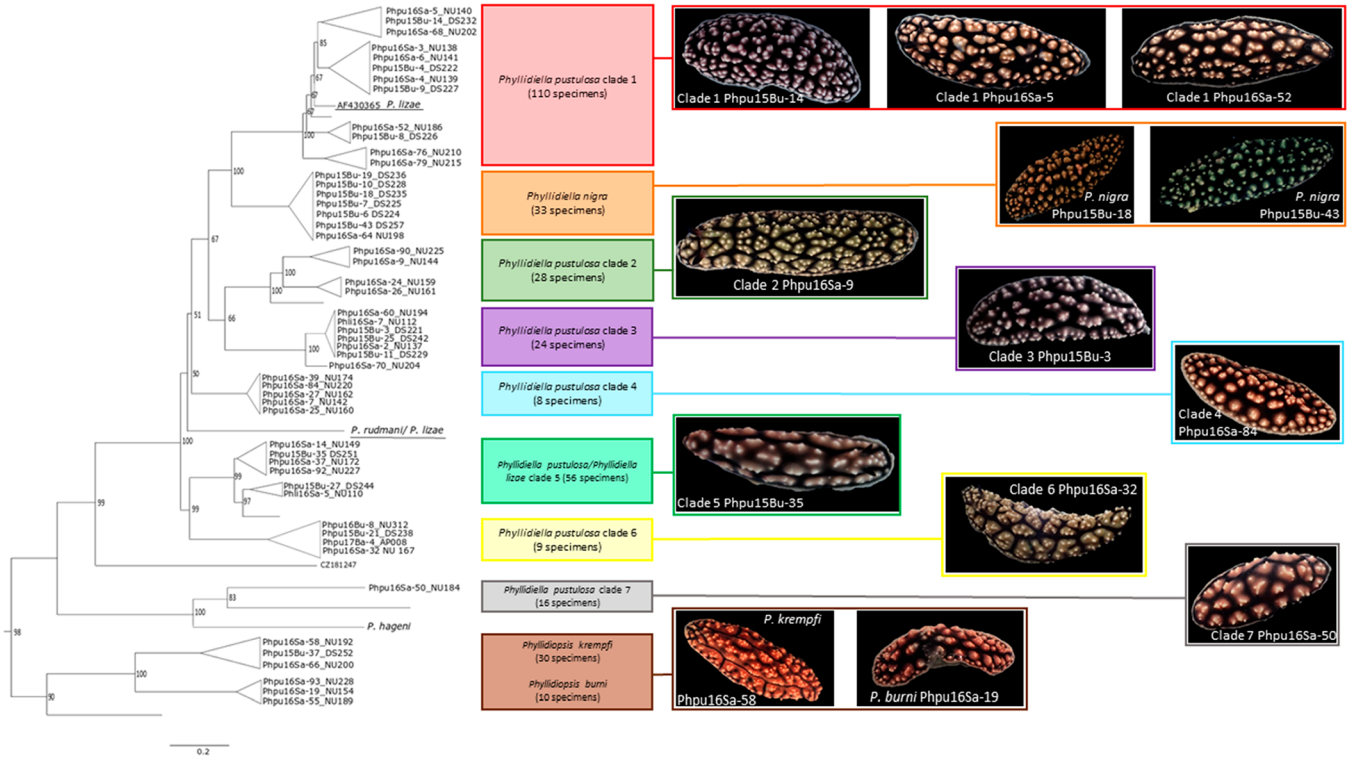

Figure 1. Condensed phylogenetic tree including the chemically investigated 52 phyllidiid specimens. The tree reconstruction, based on 16S and CO1 partial gene sequences, includes 340 *Phyllidiella* and *Phyllidiopsis* specimens (our own and from NCBI). Clades are partly collapsed and shown as triangles to increase clarity. Numbers within the colored clades indicate the number of specimens used for tree reconstruction. The distinct *P. pustulosa* clade 6 (yellow frame) possesses unique chemotype, and the specimen Phpu15Bu-21 was chemically analyzed in detail for its secondary metabolites. Bu in the identifier signifies Bunaken National Park as locality, Ba = Bangka Island, and Sa = Sangihe Island.

noted in *P. pustulosa* by Okino and co-workers,[19] who compared four populations from different sites and found different terpenoid compounds in each population.

In this study we provide the first results evolved from the overall phylogenetic reconstruction of more than 700 phyllidiid specimens using molecular 16S and CO1 markers and morphological characters (Papu et al., in preparation). In addition to more evidence for cryptic speciation in the various phyllidiid species and genera, this analysis confirms cryptic species within the *P. pustulosa* species complex, involving seven clades. In order to find chemical differences between the clades supporting the molecular results, we chemically analyzed 52 specimens of these seven distinct clades, as well as the closely related species *P. nigra*, *Phyllidiopsis burni*, and *P. krempfi*. These analyses provided results that, interestingly, highlighted one clade specifically, from which we report the isolation and structure elucidation of seven new dichloroimidic sesquiterpenoids and their derivates (**1**–**7**) and a structure assignment of two unstable dichloroimidic sesquiterpenoids (**8**, **9**).

RESULTS AND DISCUSSION

During several expeditions to Bunaken National Park, Bangka Archipelago, and Sangihe Island (North Sulawesi, Indonesia) between 2015 and 2018, more than 500 phyllidiid specimens were collected.[11,29−31] Based on morphological inspection in the field, 269 specimens of these were tentatively identified as *Phyllidiella pustulosa*. A tree of the Phyllidiidae, including these specimens, was retrieved from two mitochondrial genes (16S and CO1 partial gene sequences), including sequences from NCBI (Papu et al., in preparation). The phylogenetic analysis revealed the species *P. pustulosa* as a species complex and thus confirms previous studies.[10] *P. nigra* and *P. rudmani* cluster within *P. pustulosa* clades, additionally rendering *P. pustulosa* a paraphyletic group (Figure 1). Specimens assigned to *P. lizae* (Table 1) also cluster with *P. pustulosa* specimens from clade 1 and clade 5, as well as *P. rudmani*. These results clearly indicate the necessity of a revision of systematics within the genus *Phyllidiella*. Figure 1 highlights (in colored boxes) all *P. pustulosa* clades including specimens from the closely related genus *Phyllidiopsis*, of which selected specimens were also chemically analyzed during this project. Based on this phylogenetic reconstruction, 52 specimens representing all seven clades of *P. pustulosa* (including specimens with atypical color variations, thus probably misidentified in the field) and closely related *P. nigra* and *Phyllidiopsis* spp. were selected (see identifiers in Figure 1) and subjected to metabolomic analysis.

Extracts of individually stored nudibranchs were first analyzed by ^{1}H NMR spectroscopy and HR-LCMS. The occurrence of several chemotypes became evident after the preliminary ^{1}H NMR analysis and was finally confirmed by HR-LCMS. Obtained MS data also allow molecular network analyses using the Web-based platform Global Natural Products Social Molecular Networking (GNPS), which provides a method to rapidly assess the diversity and chemical relatedness of secondary metabolites in complex extracts, based on similarities in MS/MS parent ion fragmentation patterns.[36] Interestingly, a locality-dependent distribution of the secondary metabolite profiles, e.g., dependent upon the prevailing food sponges, as originally hypothesized by us, was not found. Instead, the chemical profiles correlated with the results of the phylogenetic study. The metabolomic analysis using the GNPS platform clearly indicated that the specimens Phpu15Bu-21,

https://dx.doi.org/10.1021/acs.jnatprod.0c00783
J. Nat. Prod. XXXX, XXX, XXX−XXX

Table 1. List of Sequences (Own and Published Data) Used in This Study for Tree Reconstruction[10,11,32−35]

species	CO1 gene[a]	16S gene[a]	voucher/ID	locality[b]
Phyllidiella pustulosa	KX235966		336586	Southeast Gam, Desa Besir, Raja Ampat, Indonesia
Phyllidiella pustulosa	KX235969		336585	Southeast Gam, Desa Besir, Raja Ampat, Indonesia
Phyllidiella pustulosa	KX235962		336587	South Gam, Eastern entrance Besir Bay, Cape Besir, Raja Ampat, Indonesia
Phyllidiella pustulosa	KX235961		336584	West Pulau Yeben Kecil, Raja Ampat, Indonesia
Phyllidiella pustulosa	KX235964		336583	South Gam, Eastern entrance Besir Bay, Cape Besir, Raja Ampat, Indonesia
Phyllidiella pustulosa	KX235957		336474	Tanjung Tabam, Ternate, Indonesia
Phyllidiella pustulosa	KX235956		336470	Northwest side of Maitara, Ternate, Indonesia
Phyllidiella pustulosa	KX235954		336460	Desa Tahua, Ternate, Indonesia
Phyllidiella pustulosa	KX235955		336461	Desa Tahua, Ternate, Indonesia
Phyllidiella pustulosa	KX235959		336508	Dufadufa/Benteng Toloko, Ternate, Indonesia
Phyllidiella pustulosa	KX235970		336588	West Pulau Yeben Kecil, Raja Ampat, Indonesia
Phyllidiella pustulosa	KX235963		336581	South Gam, Besir Bay, Raja Ampat, Indonesia
Phyllidiella pustulosa	KX235960		336510	Dufadufa/Benteng Toloko, Ternate, Indonesia
Phyllidiella pustulosa		KP873167	KP873167	Bidong Island (Terengganu)
Phyllidiella pustulosa	KX235967		336580	Southwest Pulau Kri, Raja Ampat, Indonesia
Phyllidiella pustulosa	KX235971		336579	South Gam, Besir Bay, Raja Ampat, Indonesia
Phyllidiella pustulosa	KX235968		336582	Southwest Pulau Kri, Raja Ampat, Indonesia
Phyllidiella pustulosa	KX235953		336436	Off Danau Laguna, Ternate, Indonesia
Phyllidiella pustulosa	KX235965		336578	South Gam, Southeast Besir Bay, Raja Ampat, Indonesia
Phyllidiella pustulosa	KX235958		336495	Tanjung Ratemu (South of river), Ternate, Indonesia
Phyllidiella pustulosa	**MN248608**	**MN243996**	**Phpu16Sa-5**	**Sangihe Island, North Sulawesi, Indonesia**
Phyllidiella pustulosa	**MT478669**	**MT483964**	**Phpu15Bu-14**	**Bunaken Island, North Sulawesi, Indonesia**
Phyllidiella pustulosa	KJ001310		KJ001310	Lizard Island, Queensland, Australia
Phyllidiella pustulosa		AF430366	AF430366	Baie du Santal, Lifou, New Caledonia
Phyllidiella pustulosa		AF249232	AF249232	Baie du Santal, Lifou, New Caledonia
Phyllidiella pustulosa	**MN248610**		**Phpu16Sa-68**	**Sangihe Island, North Sulawesi, Indonesia**
Phyllidiella pustulosa	**MN248601**	**MN243991**	**Phpu16Sa-3**	**Sangihe Island, North Sulawesi, Indonesia**
Phyllidiella pustulosa	**MN248602**	**MN244006**	**Phpu16Sa-6**	**Sangihe Island, North Sulawesi, Indonesia**
Phyllidiella pustulosa	**MT478670**	**MT483965**	**Phpu15Bu-4**	**Bunaken Island, North Sulawesi, Indonesia**
Phyllidiella pustulosa	**MT478671**		**Phpu16Sa-4**	**Sangihe Island, North Sulawesi, Indonesia**
Phyllidiella pustulosa	**MT478672**	**MT483966**	**Phpu15Bu-9**	**Bunaken Island, North Sulawesi, Indonesia**
Phyllidiella pustulosa	**MN248627**	**MN243980**	**Phpu16Sa-9**	**Sangihe Island, North Sulawesi, Indonesia**
Phyllidiella pustulosa	**MN248621**	**MN244002**	**Phpu16Sa-52**	**Sangihe Island, North Sulawesi, Indonesia**
Phyllidiella pustulosa	**MN248615**	**MN243989**	**Phpu16Sa-76**	**Sangihe Island, North Sulawesi, Indonesia**
Phyllidiella pustulosa	**MN248619**	**MN243988**	**Phpu16Sa-79**	**Sangihe Island, North Sulawesi, Indonesia**
Phyllidiella pustulosa	**MN248630**		**Phpu16Sa-90**	**Sangihe Island, North Sulawesi, Indonesia**
Phyllidiella nigra	**MT478673**	**MT483967**	**Phpu15Bu-19**	**Bunaken Island, North Sulawesi, Indonesia**
Phyllidiella nigra	**MT478674**	**MT483968**	**Phpu15Bu-10**	**Bunaken Island, North Sulawesi, Indonesia**
Phyllidiella nigra	**MT478675**	**MT483969**	**Phpu15Bu-18**	**Bunaken Island, North Sulawesi, Indonesia**
Phyllidiella nigra	**MT478676**	**MT483970**	**Phpu15Bu-7**	**Bunaken Island, North Sulawesi, Indonesia**
Phyllidiella nigra	**MT478677**	**MT483971**	**Phpu15Bu-6**	**Bunaken Island, North Sulawesi, Indonesia**
Phyllidiella nigra	**MT478678**	**MT483972**	**Phpu15Bu-43**	**Bunaken Island, North Sulawesi, Indonesia**
Phyllidiella nigra	**MT478679**	**MT483973**	**Phpu16Sa-64**	**Sangihe Island, North Sulawesi, Indonesia**
Phyllidiella pustulosa	**MN248625**	**MN243978**	**Phpu16Sa-24**	**Sangihe Island, North Sulawesi, Indonesia**
Phyllidiella pustulosa	**MN248626**	**MN243979**	**Phpu16Sa-26**	**Sangihe Island, North Sulawesi, Indonesia**
Phyllidiella pustulosa	**MN248634**	**MN244014**	**Phpu16Sa-60**	**Sangihe Island, North Sulawesi, Indonesia**
Phyllidiella pustulosa	**MN248633**	**MN244013**	**Phli16Sa-7**	**Sangihe Island, North Sulawesi, Indonesia**
Phyllidiella pustulosa	**MT478680**	**MT483974**	**Phpu15Bu-3**	**Bunaken Island, North Sulawesi, Indonesia**
Phyllidiella pustulosa	**MT478681**	**MT483975**	**Phpu15Bu-25**	**Bunaken Island, North Sulawesi, Indonesia**
Phyllidiella pustulosa	**MT478682**	**MT483976**	**Phpu15Bu-11**	**Bunaken Island, North Sulawesi, Indonesia**
Phyllidiella pustulosa	**MN248636**	**MN244015**	**Phpu16Sa-2**	**Sangihe Island, North Sulawesi, Indonesia**
Phyllidiella pustulosa	**MN248638**	**MN244018**	**Phpu16Sa-70**	**Sangihe Island, North Sulawesi, Indonesia**
Phyllidiella pustulosa	**MN248598**	**MN244010**	**Phpu16Sa-39**	**Sangihe Island, North Sulawesi, Indonesia**
Phyllidiella pustulosa	**MN248599**	**MN244012**	**Phpu16Sa-84**	**Sangihe Island, North Sulawesi, Indonesia**
Phyllidiella pustulosa	**MN248596**	**MN244009**	**Phpu16Sa-27**	**Sangihe Island, North Sulawesi, Indonesia**
Phyllidiella pustulosa	**MN248594**	**MN244007**	**Phpu16Sa-7**	**Sangihe Island, North Sulawesi, Indonesia**
Phyllidiella pustulosa	**MN248595**	**MN244008**	**Phpu16Sa-25**	**Sangihe Island, North Sulawesi, Indonesia**
Phyllidiella pustulosa	**MT478683**		**Phpu15Bu-27**	**Bunaken Island, North Sulawesi, Indonesia**
Phyllidiella pustulosa	**MN248580**		**Phpu16Sa-14**	**Sangihe Island, North Sulawesi, Indonesia**
Phyllidiella pustulosa	**MN248592**	**MN243967**	**Phpu16Sa-92**	**Sangihe Island, North Sulawesi, Indonesia**
Phyllidiella pustulosa	**MT478684**	**MT483977**	**Phpu15Bu-35**	**Bunaken Island, North Sulawesi, Indonesia**

https://dx.doi.org/10.1021/acs.jnatprod.0c00783
J. Nat. Prod. XXXX, XXX, XXX−XXX

Table 1. continued

species	CO1 gene[a]	16S gene[a]	voucher/ID	locality[b]
Phyllidiella pustulosa	**MT478685**	**MT483978**	**Phpu16Sa-37**	**Sangihe Island, North Sulawesi, Indonesia**
Phyllidiella pustulosa	**MT478686**	**MT483979**	**Phpu16Bu-8**	**Bunaken Island, North Sulawesi, Indonesia**
Phyllidiella pustulosa	**MT478687**	**MT483980**	**Phpu15Bu-21**	**Bunaken Island, North Sulawesi, Indonesia**
Phyllidiella pustulosa		**MT483981**	**Phpu17Ba-4**	**Bangka Island, North Sulawesi, Indonesia**
Phyllidiella pustulosa		**MT483982**	**Phpu16Sa-32**	**Sangihe Island, North Sulawesi, Indonesia**
Phyllidiella pustulosa	**MN248641**	**MN243958**	**Phpu16Sa-50**	**Sangihe Island, North Sulawesi, Indonesia**
Phyllidiella nigra	KX235948		336472	Maitara Northwest, Ternate, Indonesia
Phyllidiella nigra	KX235949		336501	Sulamadaha I, Ternate, Indonesia
Phyllidiella nigra	KX235946		336434	Off Danau Laguna, Ternate, Indonesia
Phyllidiella nigra	KX235947		336471	Maitara Northwest, Ternate, Indonesia
Phyllidiella nigra	KX235952		336576	South Gam, Eastern entrance Besir Bay, Pulau Bun, Raja Ampat, Indonesia
Phyllidiella nigra	KX235951		336577	South Gam, Southeast Besir Bay, Raja Ampat, Indonesia
Phyllidiella nigra	KX235950		336505	Sulamadaha II, Ternate, Indonesia
Phyllidiella nigra		MF958280	CASIZ186196A	Maricaban Strait, Batangas Prov. Luzon,Philippines
Phyllidiella lizae	KJ001309		KJ001309	Lizard Island, Queensland, Australia
Phyllidiella lizae		AF430365	AF430365	Baie du Santal, Lifou, New Caledonia
Phyllidiella lizae		KJ018918	KJ018918	Lizard Island, Queensland, Australia
Phyllidiella lizae	**MN248576**	**MN243972**	**Phli16Sa-5**	**Sangihe Island, North Sulawesi, Indonesia**
Phyllidiella rudmani	KX235945		336589	Southeast Gam, Friwen Wonda, Raja Ampat, Indonesia
Phyllidiopsis fissuratus	KX235944		336590	Yenweres Bay, Raja Ampat, Indonesia
Phyllidiopsis krempfi	**MN248650**	**MN244074**	**Phpu16Sa-58**	**Sangihe Island, North Sulawesi, Indonesia**
Phyllidiopsis krempfi	**MN248647**	**MN244073**	**Phpu16Sa-66**	**Sangihe Island, North Sulawesi, Indonesia**
Phyllidiopsis krempfi	KX235976		336512	Dufadufa/Benteng Toloko, Ternate, Indonesia
Phyllidiopsis krempfi	KX235974		336466	Tanjung Ebamadu, Ternate, Indonesia
Phyllidiopsis krempfi	KX235972		336453	Kampung Cina/Tapak 2, Ternate, Indonesia
Phyllidiopsis krempfi	KX235984		336595	Southwest Pulau Kri, Raja Ampat, Indonesia
Phyllidiopsis krempfi	KX235979		336594	Southwest Pulau Kri, Kuburan, Raja Ampat, Indonesia
Phyllidiopsis krempfi	KX235983		336596	Northwest Pulau Mansuar, Lalosi reef, Raja Ampat, Indonesia
Phyllidiopsis krempfi	KX235973		336462	Tanjung Ebamadu, Ternate, Indonesia
Phyllidiopsis krempfi	KX235975		336469	West Maitara, Raja Ampat, Indonesia
Phyllidiopsis krempfi	KP873168		KP873168	Bidong Island (Terengganu)
Phyllidiopsis krempfi	KX235982		336599	East Kri, Sorido Wall, Raja Ampat, Indonesia
Phyllidiopsis krempfi	KX235981		336600	Northeast Mansuar, Raja Ampat, Indonesia
Phyllidiopsis krempfi	KX235977		336650	Teluk Dodinga; West Karang Ngeli, Ternate, Indonesia
Phyllidiopsis krempfi	KX235980		336598	North Batanta, North Pulau Yarifi, Raja Ampat, Indonesia
Phyllidiopsis krempfi	KX235978		336597	Southwest Pulau Kri, Kuburan, Raja Ampat, Indonesia
Phyllidiopsis krempfi	**MT478688**	**MT483983**	**Phpu15Bu-37**	**Bunaken Island, North Sulawesi, Indonesia**
Phyllidiopsis burni	**MN248655**	**MN244078**	**Phpu16Sa-93**	**Sangihe Island, North Sulawesi, Indonesia**
Phyllidiopsis burni	**MN248652**		**Phpu16Sa-19**	**Sangihe Island, North Sulawesi, Indonesia**
Phyllidiopsis burni		**MN244081**	**Phpu16Sa-55**	**Sangihe Island, North Sulawesi, Indonesia**
Dendrodoris atromaculata	MF958434	MF958307	CASIZ181231	Janao Bay, Luzon, Philippines

[a]NCBI accession numbers for CO1 and 16S partial genes are provided, as well as individual sequence voucher/IDs. [b]Localities of the specimens according to published data are additionally provided. Specimens analyzed chemically in this study are highlighted in bold.

Phpu16Sa-32, and Phpu17Ba-4 possess unique chemical features (Figure 2, yellow nodes). All three specimens were collected in localities lying 40 to 200 km apart (Bunaken Island, Bangka Archipelago, and Sangihe Island) and during expeditions that took place in 2015, 2016, and 2017, respectively. Nevertheless, the metabolomic profiles of the specimens Phpu15Bu-21 and Phpu16Sa-32 were found to be identical (Figure 3), whereas the extract of the specimen Phpu17Ba-4 contained mostly derivatives/degradation products of the major compounds detected in the two above-mentioned phyllidiids. The most intriguing finding, however, was that these three specimens form the separate clade 6 (Figure 1, yellow), providing strong evidence of specific chemical profiles characteristic for the genetically distinct *P. pustulosa* clades or even separate as yet undescribed species.

Structure Elucidation of New Compounds 1−9. As outlined above, GNPS molecular networking of the extracts of 52 phyllidiid specimens indicated a unique secondary metabolome of the phylogenetically well separated clade 6 within the *P. pustulosa* species complex. Out of this clade one specimen (internal code Phpu15Bu-21) was chosen for detailed chemical analysis. Chromatographic separations using SPE and HPLC followed by 1D and 2D NMR methods led to the isolation and structure elucidation of two new dichloroimidic sesquiterpenes (**1** and **4**) and five new derivatives (**2**, **3**, **5**−**7**) thereof. Molecular structures of two additional dichloroimidic sesquiterpenes (**8** and **9**) could only be established by the interpretation of the HR-LCMS data due to their chemical instability.

Compound **1** was isolated as a colorless oil. The analysis of the mass spectrum obtained *via* an HR-ESIMS experiment revealed an isotope pattern typical for a polychlorinated compound. The molecular formula $C_{16}H_{22}Cl_3NO_2$ was established from *m*/*z* 366.064 $[M + H]^+$ and an ion resulting

https://dx.doi.org/10.1021/acs.jnatprod.0c00783
J. Nat. Prod. XXXX, XXX, XXX−XXX

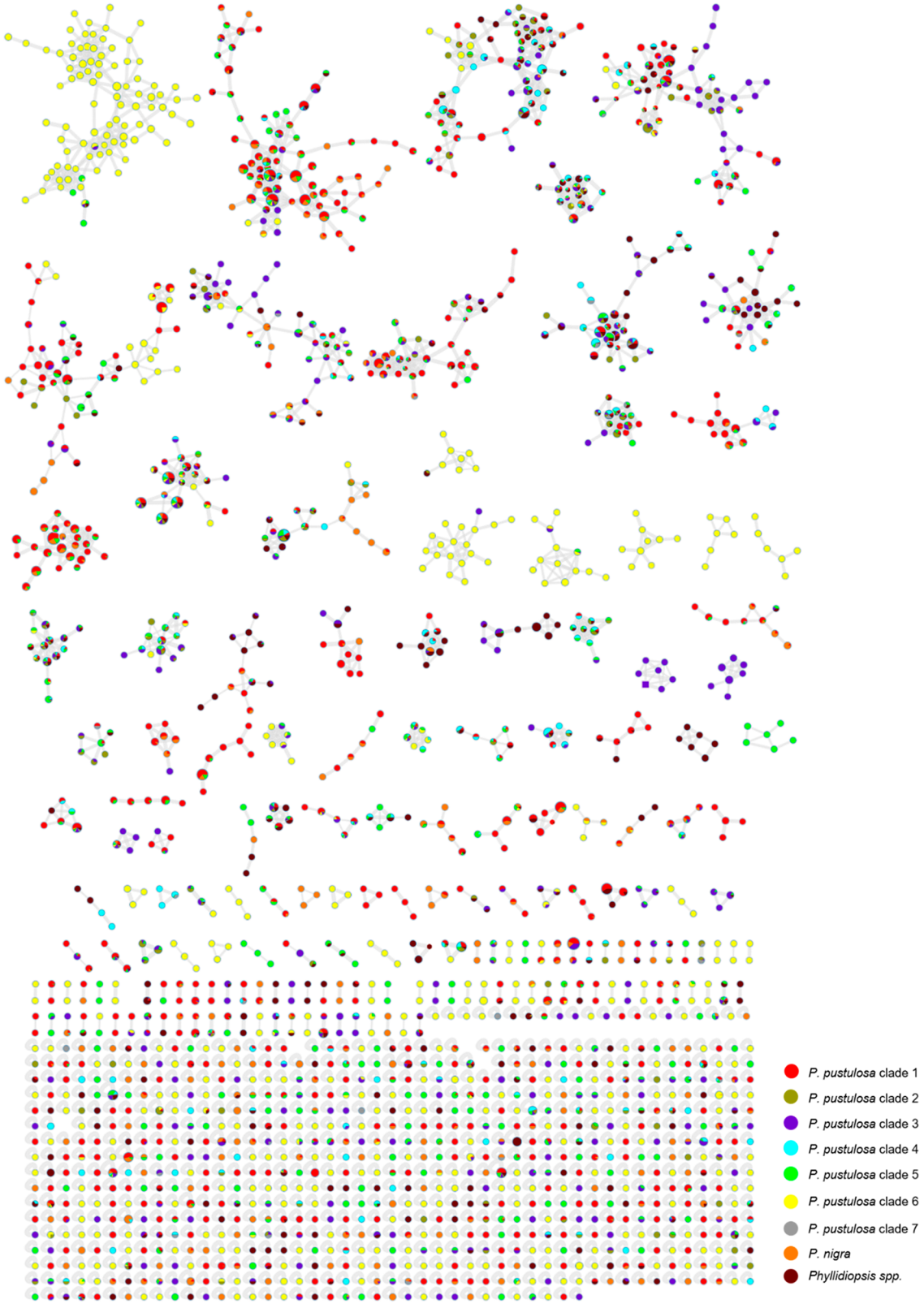

Figure 2. GNPS analysis of HR-LCMS data obtained from extracts of 52 phyllidiid specimens. Node size indicates the number of spectra (min. 1 max. 200). Nodes are color coded according to the legend and are displayed as pie charts when compounds are detected in more than one clade. Unique secondary metabolites (yellow nodes) detected in the *Phyllidiella pustulosa* clade 6 form the majority of distinct clusters.

from loss of chlorine 330.099 $[M - Cl]^+$. The molecule showed five degrees of unsaturation. The presence of the carbonimidic dichloride was evident from a strong IR absorption at 1654 cm^{-1} and a weak nonprotonated ^{13}C NMR signal at δ 127.3. The ^{13}C NMR spectrum consisted of 16 carbon resonances, which were assigned to five nonprotonated carbons, four CH, five CH_2, and three CH_3 groups using DEPT and HSQC experiments (Table 2). The presence

https://dx.doi.org/10.1021/acs.jnatprod.0c00783
J. Nat. Prod. XXXX, XXX, XXX−XXX

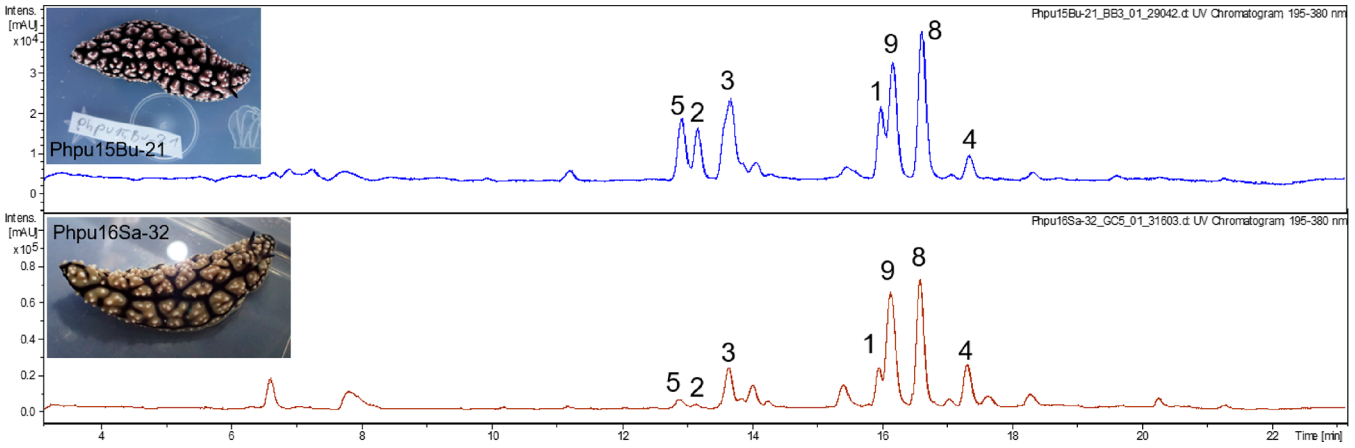

Figure 3. LC-DAD chromatograms (UV trace 195−380 nm) of two specimens phylogenetically assigned to *Phyllidiella pustulosa* clade 6. Phpu15Bu-21 and Phpu16Sa-32 were collected at different localities (Johnson diving site at Bunaken Island and Talengen Bay at Sangihe Island) about 200 km apart and in different years (2015 and 2016, respectively). Structures **1**−**9** are shown in Chart 1.

Table 2. ^{13}C and ^{1}H NMR Spectroscopic Data of Compounds 1, 2, and 4 in MeOH-d_4 ($\delta_{H/C}$ 3.35/49.0)

	1		2		4	
C[a]	δ_C[b]	δ_H (J in Hz)	δ_C[b]	δ_H (J in Hz)	δ_C[b]	δ_H (J in Hz)
1	40.9, CH_2	a 2.61, dd (6.5, 18.2) b 2.51, dd (9.5, 18.2)	40.9, CH_2	a 2.61, dd (6.5, 18.2) b 2.51, dd (9.5, 18.2)	39.8, CH_2	a 1.65, m b 1.49, m
2	219.1, C		219.1, C		26.6, CH_2	a 2.04, m b 1.72, m
3	81.9, C		81.9, C		87.7, CH	3.79, d (5.5)
4	79.1, CH	4.67, dd (6.5, 9.5)	79.1, CH	4.67, dd (6.5, 9.5)	46.4, C	
5	135.5, C		135.3, C		56.5, CH	1.38, t (8.2)
6	128.3, CH	5.66, t (6.0)	128.5, CH	5.66, br t (6.0)	88.6, C	
7	27.1, CH_2	ab 2.35, m	27.0, CH_2	ab 2.35, m	27.1, CH_2	ab 1.58, m
8	32.2, CH_2	a 2.34, m b 2.22, m	31.6, CH_2	ab 2.27, m	32.7, CH_2	ab 2.19, m
9	147.4, C		147.4, C		148.1, C	
10	63.6, CH	4.76, br t (6.8)	64.6, CH	4.55, t (7.0)	63.6, CH	4.76, t (7.0)
11	60.5, CH_2	a 3.96, dd (6.3, 14.6) b 3.90, dd (7.3, 14.6)	46.9, CH_2	a 3.54, dd (7.0, 14.5) b 3.43, dd (7.0, 14.5)	60.5, CH_2	a 3.96, m b 3.92, m
12	24.6, CH_3	1.30, s	24.6, CH_3	1.30, s	26.3, CH_3	1.15, s
13	22.2, CH_3	1.25, s	22.2, CH_3	1.25, s	23.7, CH_3	1.07, s
14	11.5, CH_3	1.73, s	11.5, CH_3	1.73, s	19.1, CH_3	1.39, s
15	115.2, CH_2	a 5.29, br s b 5.14, br s	115.1, CH_2	a 5.24, br s b 5.10, br s	114.9, CH_2	a 5.28, br s b 5.13, br s
16	127.3, C		159.0, C		127.2, C	
17			61.9, CH_2	4.11, q (7.0)		
18			14.9, CH_3	1.26, t (7.0)		

[a]All assignments are based on extensive 1D and 2D NMR measurements (COSY, HSQC, HMBC). [b]Multiplicities are determined by DEPT.

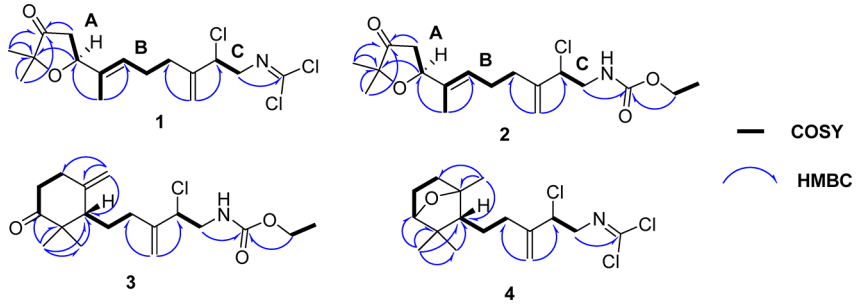

Figure 4. Key COSY and HMBC correlations in compounds **1**−**4**.

https://dx.doi.org/10.1021/acs.jnatprod.0c00783
J. Nat. Prod. XXXX, XXX, XXX−XXX

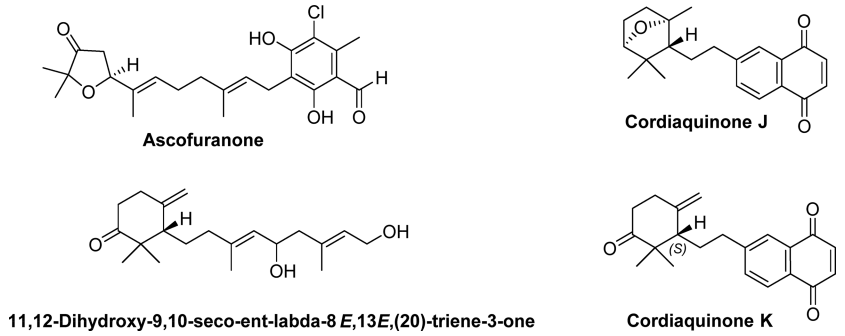

Figure 5. Natural products sharing structural similarities with the new sesquiterpenes **1**−**4**.

of four double bonds (2 C═C; 1 C═O; 1 C═N) indicated the molecule to be monocyclic. The ^{1}H NMR spectrum contained three singlet methyl signals (H_3-13, -12, -14; δ_H 1.25, 1.30, and 1.73), two broad singlet resonances at δ_H 5.29 and 5.14 that were assigned to an exomethylene group (H_2-15, δ_C 115.2), and a triplet at δ_H 5.66 (H-6, J = 6.0 Hz) attributable to an sp^2 proton. Two further deshielded resonances at δ_H 4.67 (H-4, doublet of doublets, J = 6.5, 9.5 Hz) and δ_H 4.76 (H-10, triplet J = 6.8 Hz) indicated that they are connected to a heteroatom, i.e., CH-4 to oxygen and CH-10 to chlorine. Three spin systems (**A** including H_2-1 and H-4; **B** from CH_3-14 to H_2-8, and **C** ranging from H-10 to H_2-11) were established by the interpretation of a COSY experiment (Figure 4). These ^{1}H−^{1}H spin systems were connected with each other using HMBC long-range correlations. Thus H_3-14 has a heteronuclear coupling to C-4 connecting spin systems **A** and **B**, and HMBC cross-peaks observed from the exo-methylene H_2-15 to C-8 and C-10 connected **B** with **C**. The ^{13}C NMR chemical shift (δ_C 11.5) of the resonance for the methyl C-14 demonstrated the *E* configuration of the Δ^5 double bond. Long-range CH correlations of both methyl groups CH_3-12 and CH_3-13 to each other, to C-3, and to carbonyl C-2 indicated their position on nonprotonated carbon C-3. The ^{13}C NMR resonance of C-3 at δ_C 81.9 is characteristic for the presence of an attached oxygen atom. A weak long-range correlation of H-4 to C-3 gave evidence for the oxygen bridge, and thus a dihydrofuranone ring system was established, providing the last unsaturation requirement. The presence of a chlorine atom at C-10 was delineated from a characteristic ^{13}C NMR shift of δ_C 63.6. Finally, an HMBC correlation of H_2-11 to the nonprotonated carbon C-16 indicated the position of the dichloroimidic moiety at the terminal C-11 of the C_{15} sesquiterpene skeleton and finally led to the planar structure of **1**.

Compound **2** was isolated as a colorless oil. The molecular formula $C_{18}H_{28}ClNO_4$ was established by HR-ESIMS and has five degrees of unsaturation. The dichloroimidic band at 1654 cm^{-1} was missing in the IR spectrum. Instead an additional carbonyl band appeared at 1707 cm^{-1}. ^{1}H and ^{13}C NMR spectra resembled those of **1** (Table 2). The major differences in the ^{1}H NMR spectrum were the additional signal at δ_H 4.11 (H_2-17, quartet J = 7.0 Hz) and an additional triplet signal of a methyl group at δ_H 1.26 (H_3-18, J = 7.0 Hz), indicating the presence of an ethoxy functionality. The ^{13}C NMR resonance of the dichloroimidic carbon could not be observed. Instead, an additional carbonyl signal at δ_C 159.0 for C-16 was detected. While the remaining ^{1}H and ^{13}C NMR resonances corresponded with those of the dihydrofuranone **1**, the differences mentioned above led us to conclude that we had an EtOH degradation product of **1**, because the dichloroimidic moiety is highly reactive. An HMBC experiment revealed a long-range correlation of H_2-11 and ethoxy H_2-17 to the carbonyl carbon C-16, and thus compound **2** is the ethyl carbamate of dihydrofuranone dichloroimide **1**.

C-4 Absolute Configurations of Dihydrofuranones 1 and 2. Whereas the eastern part of the compound **1** and its ethyl carbamate derivative **2** is typical for the rare dichloroimidic sesquiterpenes from marine sponges[27,37] and the phyllidiid nudibranch *Reticulidia fungia*,[38] the western part is structurally identical to that of the fungal metabolite ascofuranone (Figure 5).[39,40]

The absolute configuration of ascofuranone was established in 1975 using X-ray crystallography.[41] For the assignment of the configuration at carbon C-4, first NOESY data analysis (Figure 6) and comparison of NMR spectroscopic data of **1**

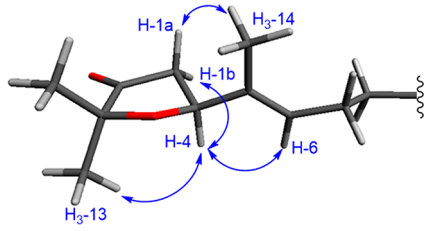

Figure 6. Relative configuration of the dihydrofuranone moiety in compounds **1** and **2**. Blue arrows indicate key NOESY correlations. The 3D model was constructed with Avogadro 1.20.

and **2** with those of ascofuranone was undertaken. The *S* configuration at C-4 in ascofuranone causes a negative Cotton effect at 300 nm as predicted by the ketone octant rule. Due to the instability of the dichloroimide **1**, circular dichroism (ECD) measurement was performed on the dihydrofuranone carbamate **2** and demonstrated a significant negative Cotton effect at 300 nm. Considering the same biosynthetic origins of both compounds **1** and **2**, the *S* configuration was assigned at C-4, as found in ascofuranone. The ^{13}C NMR data of the dihydrofuranone moiety of compounds **1** and **2** are identical and match perfectly those published for ascofuranone isolated from the sponge-derived fungus *Acremonium* sp.[42] The configuration at the chlorine bearing C-10 remains to be solved in all herein described compounds.

Compound **3** was isolated as a colorless oil with a specific rotation of $[\alpha]^{25}_{D}$ +4 (*c* 0.09, acetone). A group of isotopic signals with a characteristic pattern for a monochlorinated organic molecule with the most intense one at *m*/*z* 342.184 $[M + H]^+$ was observed in the HR-ESIMS spectrum. The molecular formula was established as $C_{18}H_{28}ClNO_3$ with five

https://dx.doi.org/10.1021/acs.jnatprod.0c00783
J. Nat. Prod. XXXX, XXX, XXX−XXX

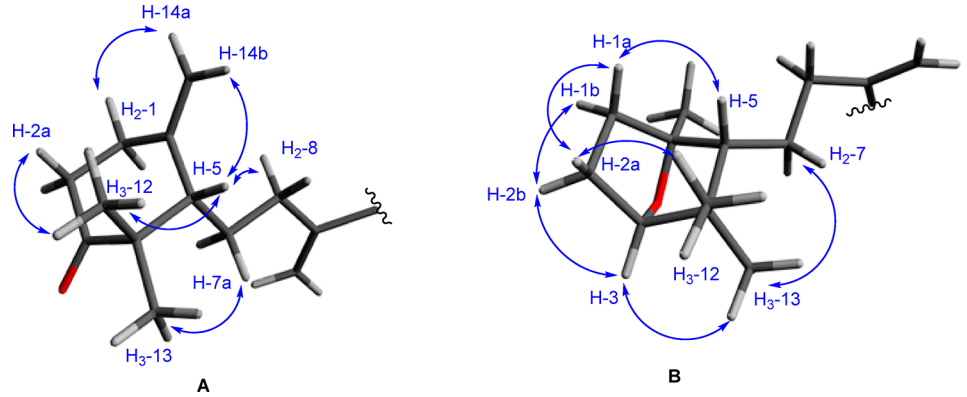

Figure 7. Configuration of the cyclic moieties. (A) As found in compound **3**. (B) As found in compound **4**. Blue arrows indicate key NOESY correlations. The 3D model was constructed with Avogadro 1.20.

degrees of unsaturation. A characteristic dichloroimidic band at 1654 cm^{-1} was missing in the IR spectrum, instead of a strong carbonyl band at 1707 cm^{-1}, indicated, as in the case of **2**, a degradation of the dichloroimidic moiety. The planar structure of **3** could be established by the analysis and comparison of 1D and 2D NMR data. ^{1}H and ^{13}C NMR spectra of compound **3** shared many similarities with those of sesquiterpene **2**, and it was found that the molecules are identical from C-18 to C-15. For the remaining part of the structure $^{1}H-^{1}H$ NMR spin systems from H-5 to H_2-7 to H_2-8 and from H_2-1 to H_2-2 and H_2-14 were detected. These fragments were then connected via HMBC correlations from the exomethylene groups H_2-15 to C-8 and H_2-14 to C-5. The two geminal methyls CH_3-12 and CH_3-13 had long-range couplings with the quaternary C-4, tertiary C-5, and the carbonyl C-3 (δ_C 217.5). The HMBC correlation of H_2-2 with the carbons C-3 and C-4 led to the formation of the cyclohexanone moiety and finally the whole planar structure of **3** (Figure 4).

Compound **4** showed a specific rotation of $[\alpha]^{25}_{D}$ +24 (*c* 0.08, acetone). An HR-ESIMS measurement in the positive mode revealed a protonated molecule having an *m/z* 352.096 $[M + H]^+$, which was part of a group of low-intensity peaks with a diagnostic isotope pattern of a molecule bearing three chlorine atoms. MS signals with higher intensity were observed with *m/z* 334.088 $[M - H_2O]^+$ and *m/z* 316.119 $[M - Cl]^+$. The molecular formula was calculated to be $C_{16}H_{24}Cl_3NO$ with four degrees of unsaturation. The IR spectrum showed a characteristic band at 1654 cm^{-1} resulting from a dichloroimidic function. The NMR spectroscopic data of compound **4** partially resembled those of **1**, indicating that the eastern parts of the molecules, i.e., from the C-15 methylene function to C-16, were identical. Compared to compound **3**, the lack of a carbonyl group next to the geminal methyls CH_3-12 and CH_3-13 was most obvious. Instead, these methyl groups exhibited HMBC correlations to tertiary carbon C-3 with a ^{13}C NMR resonance at δ_C 87.7 that clearly indicated its connection with an oxygen atom. HMBC correlations were also detected between CH_3-12 and CH_3-13 to the tertiary carbon C-5 and the quaternary carbon C-4. Methyl group CH_3-14 was located at the oxygen-bearing nonprotonated carbon (C-6, δ_C 88.6) and exhibited HMBC long-range couplings to both C-5 and C-1. A COSY spin system ranging from H_2-1 via H_2-2 to H-3 enabled together with the above-mentioned HMBC correlations the deduction of a cyclohexane ring. The oxygen bridge between C-3 and C-6 was evident due to a long-range HMBC coupling of H-3 with C-6. An additional $^{1}H-^{1}H$ spin system from H-5 via the methylene groups H_2-7 to H_2-8 and a clear HMBC correlation of the methylene protons H_2-15 to carbon C-8 connected the ring with the eastern part and completed the structure.

Compound **5** was only detected as part of a mixture together with compound **3**. LC-HRMS (Supporting Information Figure S26) analysis of this mixture showed the presence of compound **3**, as well as signals for a compound with an *m/z* 344.198 $[M + H]^+$. This MS result was indicative for the presence of two additional hydrogens in **5**. The formula was thus established as $C_{18}H_{30}ClNO_3$ with four degrees of unsaturation. The planar structure of **5** was elucidated unambiguously basing on 1D and 2D NMR experiments after the subtraction of the signals that were already assigned to compound **3**. The only major differences between **3** and **5** were found in the cyclohexane ring. NMR signals for the carbonyl group C-3 were missing in **5**, and instead an additional signal appeared in the ^{1}H NMR spectrum (δ_H 3.40, m) that exhibited an HSQC to an oxygen bearing carbon (δ_C 77.8) indicating the reduction of the ketone to a secondary alcohol. Compound **5** seems to convert to **3** under chromatographic separation conditions; thus, repeated attempts to isolate **5** as a pure compound were unsuccessful.

Compounds **6** and **7** were also isolated in a mixture after repeated HPLC separations. Careful inspection of the NMR and MS data indicated that they are the methyl carbamate derivatives of compounds **3** and **5**. Most indicative were HMBC correlations of the C-17 methoxy group resonances at δ_H 3.66 and 3.67, respectively, to the carbonyl carbon at δ_C 159.4 (C-16). Remaining ^{1}H and ^{13}C NMR shifts corresponded with those of **3** and **5**.

Configurations of Compounds 3−7. The configuration of the cyclic part of the molecules was established by the interpretation of NOESY data, circular dichroism, molecular modeling, and comparison of spectroscopic data with those of similar compounds from the literature (Figure 5), *i.e.*, secolabdanes[43] and cordiaquinones J and K.[44] The cyclohexanone moieties of compounds **3** and **6** possess one stereogenic carbon, i.e., the tertiary C-5. To depict the conformation of the cyclohexanone structure and its relative configuration, minimal energy conformer searches using the Avogadro software version 1.20[45] combined with the analysis of the NOESY spectra were performed. NOE correlations between proton H-14b and H-5 and between H-5 and both the methyl group H_3-12 and the methylene group H_2-8 can only be explained with the pseudoaxial orientation of the side chain (Figure 7).

https://dx.doi.org/10.1021/acs.jnatprod.0c00783
J. Nat. Prod. XXXX, XXX, XXX−XXX

Chart 1. Structures of the New Metabolites from *Phyllidiella pustulosa* (Phpu15Bu-21) Clade 6

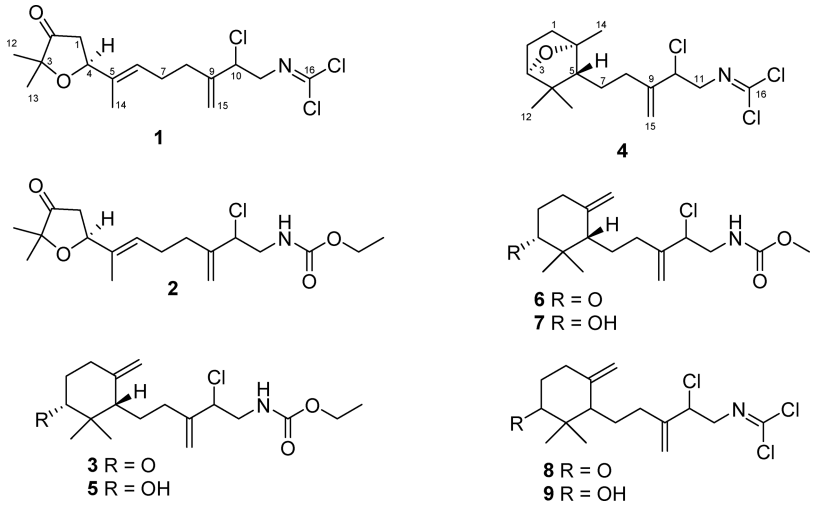

Additionally, an ECD measurement of compound **3** revealed a positive Cotton effect at 300 nm, indicating the *S* configuration at C-5, in accordance with the observations for the seco-labdane by Zdero and co-workers.[43]

As described in the literature the cyclohexane moiety in the western part of compound **4** has a preferred boat conformation due to the oxygen bridge.[44] The assignment of the relative configuration of the oxabicyclo ring system using NOESY is not straightforward. NOE correlations between H-5 and H-1a, between H-1a and H-2a, and between H-2a and H_3-12 indicated the same pseudoaxial orientation of protons H-1a, H-2a, H-5, and H_3-12. The bulky side chain at C-5 thus has an energetically favored pseudoequatorial orientation, which is further confirmed by a clear NOE correlation of H_3-13 with H_2-7. The ^{13}C NMR shifts of the whole oxabicyclo moiety of compound **4** are identical with the reported values for cordiaquinone J,[44] demonstrating the same relative configuration of both natural products. Yajima and co-workers synthesized different enantiomers of cordiaquinone J and provided NMR data of them confirming the relative configuration of the natural cordiaquinone J.[46] Considering the same biosynthetic origin of compounds **3** and **4**, the same spatial orientation of the substituents at C-5 is very likely. We thus suggest the absolute configuration of the oxabicyclic moiety in compound **4** to be 3*R*, 5*R*, 6*S*.

Because the cyclohexanones (**3** and **6**) and their cyclohexanol counterparts co-occur and moreover seemingly interconvert, the same configuration at C-5 is very likely. Considering the *R* configuration of C-5, the configuration of the hydroxy group bearing carbon C-3 could be established by an NOE correlation between H-3 and H-5 observed for compound **7**, demonstrating the spatial orientation to the same face. Thus, the configuration of cyclohexanols **5** and **7** is 3*S*, 5*R*.

Assignment of the Structures 8 and 9. The analysis of the HR LCMS data of the extract of the herein investigated *P. pustulosa* specimen pointed toward the presence of two additional major metabolites. However, they could not be isolated by chromatographic means. ^{1}H and ^{13}C NMR analysis of the initially collected fraction SPE3 HPLC2 in the course of the preparative HPLC showed that the fraction contained several substances. Repeated HPLC was performed and resulted in the isolation of an inseparable mixture of the artifacts **6** and **7** that were formed during chromatography or the NMR measurement in deuterated MeOH (as seen in the LC HRMS analysis). The original natural products are highly reactive and quickly degrade during the workup procedure.

Combining the knowledge obtained during the identification of the structures of **1**−**7** and a detailed analysis of MS data obtained in the course of our initial LC HRMS measurements of the Phyllidiid extracts enabled the structure assignment for metabolites **8** and **9**. Prominent HPLC peaks with retention times of 16.1 and 16.6 min (Figure 2, Figures S34−S36) revealed the characteristic isotopic patterns of polychlorinated compounds, indicating the presence of the dichloroimidic moiety. The *m/z* values of 350.081 $[M + H]^+$ and 314.103 $[M - HCl]^+$ found for the HPLC peak at t_R 16.6 min were attributable to a compound with a molecular formula of $C_{16}H_{24}Cl_3NO$. The HPLC peak at 16.1 min led to *m/z* values of 352.095 $[M + H]^+$, 334.086 $[M + H - H_2O]^+$, and 316.122 $[M - HCl]^+$ that was deduced as a molecular formula of $C_{16}H_{26}Cl_3NO$. These formulas are attributable to the sesquiterpenoids with the same core structure as found for compounds **3**, **5**, **6**, and **7**, but in the case of **8** and **9** with an intact dichloroimidic moiety instead of carbamates. Thus, compound **8** is a cyclohexanone (t_R 16.6 min) and **9** is its corresponding alcohol, eluting earlier from the RP stationary phase (at 16.1 min).

This study led to the identification of the structurally intriguing dichloroimidic sesquiterpenoids **1**, **4**, **8**, and **9** along with the solvent artifacts **2**, **3**, and **5**−**7** thereof (Chart 1) in a distinct phylogenetic clade of the *P. pustulosa* species complex. The presence of chlorine and the dichloroimidic moiety in these molecules allows their specific detection by MS, via the characteristic isotopic as well as fragmentation patterns, directly from extracts of the nudibranchs. However, no further dichloroimides could be detected in any other *P. pustulosa* clade nor in any other phyllidiid species chemically analyzed using HR-LCMS in the course of this study (partially unpublished data: *Phyllidia varicosa*, *P. elegans*, *P. ocellata*, *Phyllidiella lizae*, *P. nigra*, *Phyllidiopsis burni*, *P. krempfi*, *and P. shireenae*). This observation leads to the conclusion, that dichloroimidic sesquiterpenoids and their derivatives formed under the influence of solvents during the workup (**1**−**9**) represent a unique chemotaxonomic feature of *Phyllidiella pustulosa* clade 6.

https://dx.doi.org/10.1021/acs.jnatprod.0c00783
J. Nat. Prod. XXXX, XXX, XXX−XXX

Natural products containing a dichloroimidic moiety are extremely rare, although the first ones were isolated in the late 1970s from the Indo-Pacific sponge *Pseudaxinyssa pitys* (accepted now as *Axinyssa mertoni*[47]) by Faulkner and coworkers.[48,49] Despite their early discovery at the very beginning of research on marine natural products, there are only 16 metabolites bearing this functionality known to date, all derived from marine sponges and their nudibranch predators.[27] Biogenetically, the dichloroimidic functionality originates from the corresponding isocyanates and isothiocyanates, as demonstrated by incubation experiments with ^{14}C-labeled precursors in the tropical marine sponge, *Stylotella aurantium*.[50,51]

The presence of dichloroimidic compounds **1**, **4**, **8**, and **9** in extracts of animals of only one clade, i.e., clade 6 (Figure 1), indicates that speciation processes may be based on food priority. Members of this clade were found at all three collection sites (Bunaken National Park, Bangka Archipelago, and Sangihe Island). Phylogenetic analyses provided evidence for further cryptic species within the *P. pustulosa* complex, with clades usually found in all three locations, but with one exception, clade 2. The specimens within this latter clade were all only collected around Sangihe Island. Although sampling is still limited with regard to specimens in the various populations, the confinement of clade 2 to only Sangihe Island could indicate a restricted gene flow based on different larval development (with low, if at all, dispersal by free swimming larvae). However, it can also not be excluded that specific food availability (here probably an unknown sponge) restricts distribution of this clade.

Within this study we show that results of chemical and molecular phylogenetic analyses support each other, demonstrating that subclades within the *P. pustulosa* complex are in part also characterized by different chemical constituents. *P. pustulosa* was already recognized as a species complex,[10] and our studies even go further, by not only showing this species as a complex of several distinct clades but also the clustering of known and described species (*P. nigra*, *P. rudmani*, *P. lizae*) within the *P. pustulosa* complex.

The absence of clear morphologically characterizing features renders this very common nudibranch taxon, characterized by the presence of unusual natural products, an extremely difficult group with regard to correct taxonomic identification. A revision of the genus is warranted and needs to include more species than those involved in our study. Phyllidiid nudibranchs sequester the secondary metabolites from sponges; however not much is known about the preferences toward a certain favored prey. The presence of different metabolomes in sympatrically living "species" indicates that at least some of the Phyllidiidae like *P. pustulosa* clade 6 appear to be highly specialized feeders. The ongoing speciation process is thus mainly driven by food that provides the specific compounds. Providing information on clade-specific metabolomic markers, chemotaxonomic analyses might help in solving the *P. pustulosa* conundrum and strengthen the hypotheses of different species being present in one visually nearly identical group as we have shown here for clade 6.

EXPERIMENTAL SECTION

General Experimental Procedures. Optical rotations were measured with a Jasco P-2000 polarimeter. UV and IR spectra were obtained using PerkinElmer Lambda 40 and PerkinElmer Spectrum BX instruments, respectively. ECD spectra were taken on a Jasco J-810 CD spectropolarimeter. All NMR spectra were recorded in MeOH-d_4 using Bruker Avance 300 DPX or Bruker Ascend 600 spectrometers. Spectra were referenced to residual solvent signals with resonances at $\delta_{H/C}$ 3.35/49.0. Mass spectra were recorded on a micrOTOF-QIII mass spectrometer (Bruker) with an ESI-source coupled with an HPLC Dionex Ultimate 3000 (Thermo Scientific) using an EC10/2 Nucleoshell C_{18} 2.7 μm column (Macherey-Nagel). The column temperature was 25 °C. MS data were acquired over a range from 100 to 3000 m/z in positive mode. Auto MS/MS fragmentation was achieved with rising collision energy (35−50 keV over a gradient from 500 to 2000 m/z) with a frequency of 4 Hz for all ions over a threshold of 100. HPLC begins with 90% H_2O containing 0.1% acetic acid. The gradient starts after 1 min to 100% CH_3CN (0.1% acetic acid) in 20 min. A 5 μL amount of a 1 mg/mL sample solution (MeOH) was injected at a flow of 0.3 mL/min. All solvents were LCMS grade. Preparative HPLC was performed on a Merck Hitachi HPLC system equipped with an L-6200A pump, an L-4500A PDA detector, a D-6000A interface with D-7000A HSM software, and a Rheodyne 7725i injection system. A Nucleodur C_{18} 5 μm Pyramid 250 mm × 10 mm (Macherey-Nagel) and a Kinetex PFP 5 μm C_{18} 100 Å 250 mm × 4.6 mm (Phenomenex) column were used.

Samples. The animals for the chemical analyses were collected in 2015 to 2017 in the course of the biodiversity survey around North Sulawesi by Nani Undap, Adelfia Papu, and collaborators (Eisenbarth et al. 2018, Undap et al. 2019, Papu et al. 2020).[11,30,31] The collections are registered at UNSRAT collection under the numbers SRU2015/01, SRU2016/01, SRU2016/02, and SRU2017/01. The specimens were fixed individually in EtOH (96%) immediately after the collection and preliminary identification. After the transfer to University of Bonn samples were stored at −20 °C until extraction and further processing.

Extraction and Isolation. The ethanolic storage solution was decanted and evaporated under reduced pressure. The bodies were cut into small pieces and repeatedly extracted with MeOH (3 × 30 mL) and CH_2Cl_2 (1 × 30 mL). The fractions were combined to give the crude extract. HR-LCMS analysis was performed using a 1 mg/mL LCMS-grade MeOH solution of the crude extracts.

The extract of the specimen Phpu15Bu-21 was submitted for further detailed chemical analysis. The extract (300 mg) was resuspended in 30 mL of H_2O and extracted three times with 30 mL of EtOAc in a 100 mL separation funnel. The obtained lipophilic part (56.6 mg) underwent fractionation on a reversed-phase SPE Bakerbond 2000 mg column using a stepwise gradient (50:50, 70:30, 90:10, 100:0 MeOH/H_2O v/v, 20 mL each) to obtain four fractions. The fifth fraction was eluted with 20 mL of acetone. ^{1}H NMR experiments demonstrated that SPE fractions 2 (4 mg) and 3 (25 mg) were identical. They were combined and submitted to HPLC separation using the Nucleodur C_{18} 5 μm Pyramid 250 mm × 10 mm column and 85:15 MeOH/H_2O mobile phase at 2.5 mL/min flow to yield four fractions, two of which were already pure compounds (compound **1**, 1.3 mg; compound **4**, 1.1 mg). Repeated HPLC of the remaining fractions using the same column with a 75:25 MeOH/H_2O mobile phase and the analytical column Kinetex PFP 5 μm C_{18} 100 Å 250 mm × 4.6 mm with a 68:32 MeOH/H_2O mobile phase at 0.7 mL/min flow resulted in the isolation of pure compounds **2** (0.8 mg) and **3** (1.0 mg) as well as poorly separable mixtures containing compounds **3** and **5** (1.5 mg) and **6** and **7** (2.0 mg).

Compound ***1:*** colorless oil, $[\alpha]^{25}_D$ −32 (*c* 0.1, acetone); IR (neat) ν_{max} 2928, 1755, 1654, 1172, 1112, 883 cm^{-1}; ^{1}H NMR and ^{13}C NMR data, Table 2; HR-ESIMS m/z 330.099 $[M - Cl]^+$ (calcd for $C_{16}H_{22}Cl_2NO_2$, 330.102).

Compound ***2:*** colorless oil, $[\alpha]^{25}_D$ −15 (*c* 0.1, $CHCl_3$); ECD (2.8 mM, CH_3CN) λ ($\Delta\varepsilon$) 210 (+0.27), 310 (−0.11); IR (neat) ν_{max} 2926, 2854, 1754, 1707, 1526, 1457, 1376, 1252, 1172, 1112, 1030 cm^{-1}; ^{1}H NMR and ^{13}C NMR data, Table 2; HR-ESIMS m/z 358.178 $[M + H]^+$ (calcd for $C_{18}H_{29}ClNO_4$, 358.178).

Compound ***3:*** colorless oil; $[\alpha]^{25}_D$ +4 (*c* 0.09, acetone); ECD (2.9 mM, CH_3CN) λ ($\Delta\varepsilon$) 310 (+0.02); IR (neat) ν_{max} 2926, 2854, 1754, 1707, 1526, 1457, 1376, 1252, 1172, 1112, 1030 cm^{-1}; ^{1}H NMR and

https://dx.doi.org/10.1021/acs.jnatprod.0c00783
J. Nat. Prod. XXXX, XXX, XXX−XXX

^{13}C NMR data, see Table S3; HR-ESIMS m/z 342.184 $[M + H]^+$ (calcd for $C_{18}H_{29}ClNO_3$, 342.183).

Compound **4**: colorless oil; $[\alpha]^{25}_D$ +24 (c 0.08, acetone); IR (neat) ν_{max} 2928, 1733, 1654, 1456, 875 cm^{-1}; ^{1}H NMR and ^{13}C NMR data, see Table S4; HR-ESIMS m/z 352.096 $[M + H]^+$ (calcd for $C_{16}H_{25}Cl_3NO$, 352.099).

Compound **5**: isolated in a mixture with **3**; colorless oil; ^{1}H NMR and ^{13}C NMR data, see Table S5; HR-ESIMS m/z 344.198 $[M + H]^+$ (calcd for $C_{18}H_{31}ClNO_3$, 344.199).

Compounds **6** *and* **7**: isolated in a mixture; colorless oil; ^{1}H NMR and ^{13}C NMR data, see the SI.

MS Data Analysis. The obtained raw .d LCMS/MS folders were converted using the DataAnalysis 4.2 software (Bruker Daltonic) to .mzXML format and uploaded to the MassIVE server (https://massive.ucsd.edu) via FileZilla (https://filezilla-project.org) FTP client. A molecular network was created using the online workflow (https://ccms-ucsd.github.io/GNPSDocumentation/) on the GNPS Web site (http://gnps.ucsd.edu). The data were filtered by removing all MS/MS fragment ions within ±17 Da of the precursor m/z. MS/MS spectra were window filtered by choosing only the top 6 fragment ions in the ±50 Da window throughout the spectrum. The precursor ion mass tolerance was set to 0.05 Da and a MS/MS fragment ion tolerance of 0.02 Da. A network was then created where edges were filtered to have a cosine score above 0.6 and more than 3 matched peaks. Further, edges between two nodes were kept in the network if and only if each of the nodes appeared in each other's respective top 10 most similar nodes. Finally, the maximum size of a molecular family was set to 100, and the lowest scoring edges were removed from molecular families until the molecular family size was below this threshold. The spectra in the network were then searched against GNPS's spectral libraries. The library spectra were filtered in the same manner as the input data. All matches kept between network spectra and library spectra were required to have a score above 0.7 and at least 3 matched peaks. Networks were visualized using Cytoscape v3.7.2 https://cytoscape.org/.[52] Nodes attributable to the MS/MS spectra from blank samples (LCMS grade MeOH) were subtracted together with the whole clusters from the network in order to eliminate unspecific instrument noise.

Molecular Modeling. Minimal energy conformations and 3D representations of the molecules were generated using the Avogadro software version 1.20.[45]

DNA Extraction, Amplification, Sequencing, and Alignment. DNA was extracted from pieces (foot or notum) of the specimens or whole body, based on the size of animals. DNA isolation has been carried out by means of QIAgen DNeasy blood and tissue kit, following the manufacturer's instructions. Partial sequences of mitochondrial CO1 (ca. 680bp) and ribosomal 16S (ca. 650bp) were amplified by polymerase chain reaction (PCR) using the primers LCO1490-JJ (5′-CHACWAAYCATAAAGATATYGG-3′) and HCO2198-JJ (5′-AWACTTCVGGRTGVCCAAARAATCA-3′) for CO1[53] and 16Sar-L (5′-CGCCTGTTTATCAAAAACAT-3′) and 16Sbr-H (5′- CCGGTCTGAACTCAGATCACGT-3′) for 16S.[54] Amplification of CO1 was performed by an initial step (95 °C for 15 min) followed by 40 touch-down cycles of denaturation (94 °C for 35 s), annealing (55 °C for 90 s), and extension (72 °C for 90 s) with a final extension step 72 °C for 10 min. For 16S rRNA, the PCR started with an initial step (95 °C for 15 min), denaturation (94 °C for 45 s) followed by 34 touch-down cycles, annealing (56 °C for 45 s), extension (72 °C for 90 s), and final extension step at 72 °C for 10 min. PCR products were sequenced by Macrogen Europe Laboratory. GENEIOUS Pro 7.1.9 was used to extract the consensus sequence between the primer regions and checking the quality of sequences. Consensus sequences were blasted against the NCBI database for evaluation of identification (https://blast.ncbi.nlm.nih.gov/Blast.cgi). Specimen sequences together with sequences retrieved from NCBI were aligned in MAFFT Alignment, algorithm FFT-NS-2, scoring matrix 200PAM/k = 2. CO1 and 16S gene sequences were concatenated with GENEIOUS Pro 7.1.9 and used for subsequent tree analyses.

Phylogenetic Analyses. Phylogenetic reconstruction was carried out with maximum likelihood algorithms implemented in the IQ tree Web server. The following settings were applied: Ultrafast Bootstrap analyses, 1000 number of bootstraps, 1000 max iterations, 0.99 min correlation coefficient.[55] Collapsing of clades was processed using Dendroscope 3.5.10[56] and FigTree v1.4.4.[57] For the analysis within this project, only part of the tree is depicted. In total, 52 sequences of *Phyllidiella* and *Phyllidiopsis* specimens used for chemical taxonomic analyses are shown in this tree using Dendroscope version 3.5.10 to indicate the relationship of the targeted groups. The full tree will be published elsewhere.

■ ASSOCIATED CONTENT

Supporting Information

The Supporting Information is available free of charge at https://pubs.acs.org/doi/10.1021/acs.jnatprod.0c00783.

Additional information (PDF)

■ AUTHOR INFORMATION

Corresponding Author

Gabriele M. König − *Institute of Pharmaceutical Biology, University of Bonn, 53115 Bonn, Germany;* orcid.org/0000-0003-0003-4916; Email: g.koenig@uni-bonn.de

Authors

Alexander Bogdanov − *Institute of Pharmaceutical Biology, University of Bonn, 53115 Bonn, Germany; Center for Marine Biotechnology and Biomedicine, Scripps Institution of Oceanography, University of California San Diego, La Jolla, California 92093, United States*

Adelfia Papu − *Center of Molecular Biodiversity, Zoological Research Museum Alexander Koenig, 53113 Bonn, Germany; Faculty of Mathematics and Natural Sciences, Sam Ratulangi University, Manado 95115, Indonesia*

Stefan Kehraus − *Institute of Pharmaceutical Biology, University of Bonn, 53115 Bonn, Germany*

Max Cruesemann − *Institute of Pharmaceutical Biology, University of Bonn, 53115 Bonn, Germany;* orcid.org/0000-0001-6660-2715

Heike Wägele − *Center of Molecular Biodiversity, Zoological Research Museum Alexander Koenig, 53113 Bonn, Germany*

Complete contact information is available at: https://pubs.acs.org/10.1021/acs.jnatprod.0c00783

Author Contributions

#A. Bogdanov and A. Papu contributed equally.

Notes

The authors declare no competing financial interest.

■ ACKNOWLEDGMENTS

This project was partly funded by the German Federal Ministry of Education and Research (BMBF) "INDOBIO Indonesian Opisthobranchs and Associated Microorganisms−From Biodiversity to Drug Lead Discovery" with grant numbers 16GW0117K (G.K.) and 16GW0118 (H.W.). German Academic Exchange Service (DAAD) provided a grant for A.P. We thank M. Engeser for running mass spectrometry experiments and D. Reuter for help with the extraction of the specimens. C. Etzbauer, D. Schillo, and N. Undap helped in sequencing (ZFMK). We wish to express our gratitude to N. Yonow for her expert comments.

REFERENCES

(1) Wägele, H. *Org. Div. Evol.* **2004**, *4*, 175−188.
(2) Wägele, H.; Klussmann-Kolb, A. *Front. Zool.* **2005**, *2*, 1−18.
(3) Cimino, G.; Gavagnin, M. *Molluscs. From Chemo-ecological Study to Biotechnological Application*; Springer-Verlag Berlin Heidelberg, 2006.
(4) Wägele, H.; Ballesteros, M.; Avila, C. *Oceanogr. Mar. Biol.* **2006**, *44*, 197−276.
(5) Putz, A.; König, G. M.; Wägele, H. *Nat. Prod. Rep.* **2010**, *27*, 1386−1402.
(6) Avila, C.; Núñez-Pons, L.; Moles, J. In *Chemical Ecology; The Ecological Impacts of Marine Natural Products*; Puglisi, M. P., Becerro, M. A., Eds.; CRC Press/Taylor and Francis Group: Boca Raton, 2018; pp 71−163.
(7) Goodheart, J. A.; Bleidißel, S.; Schillo, D.; Strong, E. E.; Ayres, D. L.; Preisfeld, A.; Collins, A. G.; Cummings, M. P.; Wägele, H. *Front. Zool.* **2018**, *15*, 43.
(8) Cimino, G.; Ghiselin, M. T. *Chemoecology* **1999**, *9*, 187−207.
(9) Cimino, G.; Ghiselin, M. T. *Proc. Calif. Acad. Sci.* **2009**, *60*, 175−422.
(10) Stoffels, B. E. M. W.; van der Meij, S. E. T.; Hoeksema, B. W.; van Alphen, J.; van Alen, T.; Meyers-Muñoz, M. A.; de Voogd, N. J.; Tuti, Y.; van der Velde, G. *ZooKeys* **2016**, *605*, 1−35.
(11) Undap, N.; Papu, A.; Schillo, D.; Ijong, F. G.; Kaligis, F.; Lepar, M.; Hertzer, C.; Böhringer, N.; König, G. M.; Schäberle, T. F.; Wägele, H. *Diversity* **2019**, *11*, 170.
(12) Jasaimut, S.; Prapbai, S.; Tancharoen, C.; Yuenyongsawad, S.; Hannongbua, S.; Kongsaeree, P.; Plubrukarn, A. *J. Nat. Prod.* **2013**, *76*, 2158−2161.
(13) Carbone, M.; Ciavatta, M. L.; Manzo, E.; Li, X.-L.; Mollo, E.; Mudianta, I. W.; Guo, Y.-W.; Gavagnin, M. *Mar. Drugs* **2019**, *17*, 603.
(14) Fusetani, N.; Wolstenholme, H. J.; Shinoda, K.; Assai, N.; Matsunaga, S.; Onuki, H.; Hirota, H. *Tetrahedron Lett.* **1992**, *33*, 6823−6826.
(15) White, A. M.; Pierens, G. K.; Skinner-Adams, T.; Andrews, K. T.; Bernhardt, P. V.; Krenske, E. H.; Mollo, E.; Garson, M. J. *J. Nat. Prod.* **2015**, *78*, 1422−1427.
(16) Sim, D. C-M.; Wayan Mudianta, I.; White, A. M.; Wayan Martiningsih, N.; Loh, J. J. M.; Cheney, K. L.; Garson, M. J. *Fitoterapia* **2018**, *126*, 69−73.
(17) Burreson, B. J.; Scheuer, P. J.; Finer, J.; Clardy, J. *J. Am. Chem. Soc.* **1975**, *97*, 4763−4764.
(18) Yasman; Edrada, R.-A.; Wray, V.; Proksch, P. *J. Nat. Prod.* **2003**, *66*, 1512−1514.
(19) Okino, T.; Yoshimura, E.; Hirota, H.; Fusetani, N. *Tetrahedron* **1996**, *52*, 9447−9454.
(20) Kassühlke, K. E.; Potts, B. C. M.; Faulkner, D. J. *J. Org. Chem.* **1991**, *56*, 3747−3750.
(21) Hirota, H.; Okino, T.; Yoshimura, E.; Fusetani, N. *Tetrahedron* **1998**, *54*, 13971−13980.
(22) Wright, A. D. *Comp. Biochem. Physiol., Part A: Mol. Integr. Physiol.* **2003**, *134*, 307−313.
(23) Manzo, E.; Ciavatta, M. L.; Gavagnin, M.; Mollo, E.; Guo, Y.-W.; Cimino, G. *J. Nat. Prod.* **2004**, *67*, 1701−1704.
(24) Lyakhova, E. G.; Kolesnikova, S. A.; Kalinovskii, A. I.; Stonik, V. A. *Chem. Nat. Compd.* **2010**, *46*, 534−538.
(25) Jomori, T.; Shibutani, T.; Ahmadi, P.; Suzuka, T.; Tanaka, J. *Nat. Prod. Commun.* **2015**, *10*, 1913−1914.
(26) White, A. M.; Dao, K.; Vrubliauskas, D.; Könst, Z. A.; Pierens, G. K.; Mándi, A.; Andrews, K. T.; Skinner-Adams, T. S.; Clarke, M. E.; Narbutas, P. T.; Sim, D. C-M.; Cheney, K. L.; Kurtán, T.; Garson, M. J.; Vanderwal, C. D. *J. Org. Chem.* **2017**, *82*, 13313−13323.
(27) Garson, M. J.; Simpson, J. *Nat. Prod. Rep.* **2004**, *21*, 164−179.
(28) Emsermann, J.; Kauhl, U.; Opatz, T. *Mar. Drugs* **2016**, *14*, 16.
(29) Kaligis, F.; Schillo, D.; Dialao, J.; Schäberle, T. F.; Böhringer, N.; Bara, R.; Reumschüssel, S.; Eisenbarth, J.-H.; König, G. M.; Wägele, H. *Mar. Biodivers. Rec.* **2018**, *11*, 2.
(30) Eisenbarth, J.-H.; Undap, N.; Papu, A.; Schillo, D.; Dialao, J.; Reumschüssel, S.; Kaligis, F.; Bara, R.; Schäberle, T. F.; König, G. M.; Yonow, N.; Wägele, H. *Diversity* **2018**, *10*, 127.
(31) Papu, A.; Undap, N.; Armas Martinez, N.; Segre, M. R.; Datang, I. D.; Kuada, R. R.; Perin, M.; Yonow, N.; Wägele, H. *Diversity* **2020**, *12*, 52.
(32) Valdés, A. *J..Moll..Stud.* **2003**, *69*, 75−80.
(33) Cheney, K. L.; Cortesi, F.; How, M. J.; Wilson, N. G.; Blomberg, S. P.; Winters, A. E.; Umanzör, S.; Marshall, N. J. *J. Evol. Biol.* **2014**, *27*, 676−687.
(34) Alqudah, A. A.; Shahbudin, S.; Deny, S.; Hadry, N. F.; Khodzori, M. F. A.; Yusof, M. H.; Rani, M. H. *J. Teknol.* **2016**, *78*, 167−171.
(35) Hallas, J. M.; Chichvarkhin, A.; Gosliner, T. M. *R. Soc. Open Sci.* **2017**, *4*, 171095.
(36) Wang, M.; Carver, J. J.; Phelan, V. V.; Sanchez, L. M.; Garg, N.; Peng, Y.; Nguyen, D. D.; et al. *Nat. Biotechnol.* **2016**, *34*, 828.
(37) Musman, M.; Tanaka, J.; Higa, T. *J. Nat. Prod.* **2001**, *64*, 111−113.
(38) Tanaka, J.; Higa, T. *J. Nat. Prod.* **1999**, *62*, 1339−1340.
(39) Sasaki, H.; Hosokawa, T.; Sawada, M.; Ando, K. *J. Antibiot.* **1973**, *26*, 676−680.
(40) Araki, Y.; Awakawa, T.; Matsuzaki, M.; Cho, R.; Matsuda, Y.; Hoshino, S.; Shinohara, Y.; Yamamoto, M.; Kido, Y.; Inaoka, D. K.; Nagamune, K.; Ito, K.; Abe, I.; Kita, K. *Proc. Natl. Acad. Sci. U. S. A.* **2019**, *116*, 8269−8274.
(41) Ando, K.; Sasaki, H.; Hosokawa, T.; Nawata, Y.; Iitaka, Y. *Tetrahedron Lett.* **1975**, *11*, 887−890.
(42) Zhang, P.; Bao, B.; Dang, H. T.; Hong, J.; Lee, H. J.; Yoo, E. S.; Bae, K. S.; Jung, J. H. *J. Nat. Prod.* **2009**, *72*, 270−275.
(43) Zdero, C.; Bohlmann, F.; Niemeyer, H. M. *Phytochemistry* **1990**, *29*, 3247−3253.
(44) Ioset, J.-R.; Marston, A.; Gupta, M. P.; Hostettmann, K. *Phytochemistry* **2000**, *53*, 613−617.
(45) Hanwell, M. D.; Curtis, D. E.; Lonie, D. C.; Vandermeersch, T.; Zurek, E.; Hutchison, G. R. *J. Cheminf.* **2012**, *4*, 17.
(46) Yajima, A.; Saitou, F.; Sekimoto, M.; Maetoku, S.; Nukada, T.; Yabuta, G. *Tetrahedron* **2005**, *61*, 9164−9172.
(47) Van Soest, R. W. M.; Boury-Esnault, N.; Hooper, J. N. A.; Rützler, K.; de Voogd, N. J.; Alvarez, B.; Hajdu, E.; Pisera, A. B.; Manconi, R.; Schönberg, C.; Klautau, M.; Kelly, M.; Vacelet, J.; Dohrmann, M.; Díaz, M.-C.; Cárdenas, P.; Carballo, J. L.; Ríos, P.; Downey, R.; Morrow, C. C. World Porifera Database. *Pseudaxinyssa pitys* de Laubenfels, 1954. Accessed through: World Register of Marine Species at: http://www.marinespecies.org/aphia.php?p=taxdetails&id=193138 on 2019-10-17.
(48) Wratten, S. J.; Faulkner, D. J. *J. Am. Chem. Soc.* **1977**, *99*, 7367−7368.
(49) Wratten, S. J.; Faulkner, D. J.; Van Engen, D.; Clardy, J. *Tetrahedron Lett.* **1978**, *16*, 1391−1394.
(50) Brust, A.; Garson, M. J. *Tetrahedron Lett.* **2003**, *44*, 327−330.
(51) Simpson, J. S.; Brust, A.; Garson, M. J. *Org. Biomol. Chem.* **2004**, *2*, 949−956.
(52) Shannon, P.; Markiel, A.; Ozier, O.; Baliga, N. S.; Wang, J. T.; Ramage, D.; Amin, N.; Schwikowski, B.; Ideker, T. *Genome Res.* **2003**, *13*, 2498−504.
(53) Astrin, J. J.; Stüben, P. E. *Invertebr. Syst.* **2005**, *22*, 503−522.
(54) Palumbi, S.; Martin, A.; Romano, S.; McMillan, W. O.; Stice, L.; Grabowski, G. In *The Simple Fool's Guide To PCR*, version 2.0; University of Hawaii: Honolulu, HI, 2002; pp 1−45.
(55) Trifinopoulos, J.; Nguyen, L.-T.; von Haeseler, A.; Minh, B. Q. *Nucleic Acids Res.* **2016**, *44*, 232−235.
(56) Huson, D. H.; Richter, D. C.; Rausch, C.; Dezulian, T.; Franz, M.; Rupp, R. *BMC Bioinf.* **2007**, *8*, 460.
(57) Rambaut, A. *FigTree*, version 1.4.4; 2018; https://github.com/rambaut/figtree/releases/tag/v1.4.4.

https://dx.doi.org/10.1021/acs.jnatprod.0c00783
J. Nat. Prod. XXXX, XXX, XXX−XXX